Lot-to-Lot Variation in Adeno-Associated Virus Serotype 9 (AAV9) Preparations

Deirdre M. O'Connor,[1] Corinne Lutomski,[2] Martin F. Jarrold,[2] Nicholas M. Boulis,[1] and Anthony Donsante[1,*]

[1]Department of Neurosurgery, Emory University School of Medicine, Atlanta, Georgia; [2]Chemistry, Indiana University Bloomington, Bloomington, Indiana.

Viral vectors are complex drugs that pose a particular challenge for manufacturing. Previous studies have shown that, unlike small-molecule drugs, vector preparations do not yield a collection of identical particles. Instead, a mixture of particles that vary in capsid stoichiometry and impurities is created, which may differ from lot to lot. The consequences of this are unclear, but conflicting reports regarding the biological properties of vectors, including transduction patterns, suggest that this variability may have an effect. However, other variables, including differences in animal strains and techniques, make it difficult to identify a cause. Here, we report lot-to-lot variation in spinal cord gray matter transduction following intrathecal delivery of self-complementary adeno-associated virus serotype 9 vectors. Eleven lots of vector were evaluated from six vector cores, including one preclinical/Good Laboratory Practice lot. Eight of the lots, including the preclinical lot, failed to transduce the gray matter, whereas the other three provided robust transduction. The cause for this variation is unknown, but it did not correlate with vector titer, buffer, or purification method. These results highlight the need to identify the cause of this variation and to develop improved production and quality control methods to ensure lot-to-lot consistency of vector potency.

Keywords: AAV9, transduction, lot-to-lot variation, intrathecal, spinal cord

INTRODUCTION

IT IS ALL TOO common for competing biodistribution studies to report significantly different transduction profiles for adeno-associated viral (AAV) vectors. For instance, intravenous injection of self-complementary adeno-associated virus serotype 9 (scAAV9) into adult mice primarily transduced astrocytes[1] or neurons,[2] depending on the laboratory doing the study. Reports on intracerebroventricular delivery of AAV9 have described two distinct patterns of transduction, stemming from transduction differences between scAAV9 and single-stranded AAV9.[3] These potential issues go beyond AAV vectors. Goenawan and Hirai discovered that the timing of harvest of lentiviral vectors could affect the preferred cellular targets in the brain, due to the action of a cysteine protease, cathepsin K.[4] Failed attempts to reproduce a particular finding may never reach the literature, given the problems of publishing negative data but are discussed at meetings and on websites. While variability in viral lots might explain inconsistencies in transduction profiles, many other factors could be at play, including differences in animal strains, the timing of injections, the promoter and enhancer sequences used, and the training of personnel. Therefore, it is difficult to know whether the variances in results are due to inherent differences between vector preparations.

Previous studies in mice,[5] cats,[6] dogs,[7] pigs,[8] and primates,[9] including our own,[10] demonstrated that intrathecal delivery of AAV9 vectors can lead to the robust transduction of the gray matter of the spinal cord, including motor neurons. This approach had not previously been evaluated in rats. During our investigation, we discovered that scAAV9 vectors can be segregated into two distinct categories: those that are able to reach the gray matter from

*Correspondence: Dr. Anthony Donsante, Department of Neurosurgery, Emory University School of Medicine, 101 Woodruff Circle, Room 6339, Atlanta, GA 30322. E-mail: adonsan@emory.edu

DOI: 10.1089/hgtb.2019.105

the intrathecal space (penetrating) and those that are efficiently excluded from the gray matter (nonpenetrating). This issue was not specific to the core producing the vector or the vector genome that was being packaged. Our data point to a major, heretofore unrecognized problem with scAAV9 production, one that has led to a substantial waste of time and research funds for many laboratories.

MATERIALS AND METHODS

Plasmids

Plasmids encoding the genomes of scAAV9-CB-IGF1 and scAAV9-CB-GFP (pTR-CB-IGF1 and pTR-CB-GFP, respectively) were provided by Andrew Moreo of Nationwide Children's Vector Core. Each plasmid encodes inverted terminal repeats for self-complementary AAV production flanking a cytomegalovirus (CMV) early enhancer, chicken β-actin promoter, a modified SV40 late 16S intron, a bovine growth hormone polyadenylation site, and either the enhanced green fluorescent protein (eGFP) or human insulin-like growth factor 1 (IGF1) complementary DNA (cDNA). Production of the plasmids was performed by Aldevron (Fargo, North Dakota). In the course of manufacturing the plasmids, both plasmids were sequenced to confirm their identity. The sequences have been deposited into GenBank (MK225671 and MK225672, respectively).

Virus lots

Viral vectors were obtained from Nationwide Children's (Columbus, OH), the University of Florida Powell Gene Therapy Center (Gainesville, FL), the University of North Carolina Vector Core (Chapel Hill, NC), the University of Massachusetts Medical School Viral Vector Core (Worcester, MA), the Penn Vector Core (Philadelphia, PA), and SAB Technology, Inc. (Philadelphia, PA).

Vector delivery

All animal experiments were approved by the Emory University Institutional Animal Care and Use Committee (for rat and mouse studies) or the T3 Labs Institutional Animal Care and Use Committee (for pig studies). All rat experiments were conducted in Sprague-Dawley rats generated in our own colony and regularly crossed with fresh breeders from Invigo/Harlan. The animals were maintained on a 12:12-h light/dark cycle with food (LabDiet 5001; LabDiet, St Louis, MO) and tap water provided *ad libitum*.

Intrathecal vector delivery in rats was accomplished in one of two ways: intrathecal catheter threaded from the cisterna magna (CM) or lumbar puncture. The switch was made mid-study due to the risk of morbidity associated with catheter placement. In the earlier experiments, vector was delivered by threading a catheter from the CM to the lumbar level of the spinal cord. Catheters were created by inserting a 7-cm-long piece of polyethylene tubing (0.008″ inside diameter [I.D.], 0.014″ outside diameter [O.D.], Cat. No. PE-8-25; Strategic Applications, Lake Villa, IL) 1–2 mm into a 2.5-cm piece of BD Intramedic I.D. 0.38 mm, O.D. 1.09 mm PE20 tubing (Cat. No. 427405; BD, Franklin Lakes, NJ) and sealing the joint with clear nail polish. A wire was threaded into the catheter to give it stability while it was being inserted into the animal. Animals were anesthetized with isoflurane, and the depth of anesthesia was gauged by toe pinch. The surgical site was shaved and sterilized with betadine scrub. The body was placed at a right angle relative to the skull. An incision in the skin was made down the midline from the nuchal crest to approximately the C5 vertebra. The upper layer of muscle was cut along the midline, whereas the lower layers of muscle were bluntly dissected away from the midline and retracted, exposing the membrane covering the foramen magnum. Using a number 11 scalpel blade, an incision was gradually made by gently running the tip of the blade over the center of the membrane until cerebrospinal fluid (CSF) flowed out through the hole. The catheter was threaded through the hole and down the spinal cord until the adapter came to rest on the membrane. The wire was removed and a 27-gauge insulin syringe was used to inject 30 μL of vector through the catheter. A second syringe with 30 μL of sterile 0.9% NaCl was used to flush the catheter. The catheter was then removed. The muscle was closed in two layers, and the skin was sutured with 4-0 Vicryl suture. The animal was placed on a warm pad during recovery from anesthesia.

In later experiments, intrathecal vector delivery was accomplished by lumbar puncture adapted from a previous technical report.[11] The animal was anesthetized with isoflurane, and the skin around the L3 and L4 vertebrae was shaved and sterilized. A rolled paper towel was inserted beneath the animal to induce more curvature in the lower spine and create space between the lamina. A neonatal lumbar puncture needle (25-gauge$\times$1″, Cat. No. 405073; BD) was inserted between L3 and L4, causing the tail to twitch. The stylet was removed and CSF was observed to flow up into the reservoir. Thirty to 50 μL of CSF was removed and replaced with 30 μL of vector. A 1-mL syringe was then connected to the lumbar puncture needle, and the vector was displaced into the lumbar cistern. The

needle was then removed, and the skin was closed with 4-0 Vicryl suture. The animal was placed on a warm pad during recovery from anesthesia.

To perform intraparenchymal injections in the rats, 70-day-old rats were anesthetized with isoflurane, and the skin around the T12 and T13 vertebrae was shaved and sterilized. The animals were then placed in a stereotaxic frame. An incision was made down the midline, and the muscles attached to the T12 and T13 spinous processes were dissected away from the bone and retracted. A laminectomy was performed using rongeurs to expose the spinal cord unilaterally. A World Precision Instruments 10-μL NanoFil syringe with a 34-gauge needle was loaded with vector and affixed to a manual micromanipulator mounted to the stereotaxic frame. The tip of the needle was positioned 1 mm from the midline and resting on the surface of the dura. The needle was then lowered 1.3 mm to place the tip within the ventral horn. Two microliters of vector was injected over 2–3 min, and then, the needle was left in place for 1 min before slowing being retracted. The needle was then positioned 5 mm caudal to the first injection and the process was repeated. The muscle and skin were closed with 4-0 Vicryl suture. The animal was placed on a warm pad during recovery from anesthesia.

Intrathecal vector delivery in the pig was performed as previously described.[10] Briefly, the animal was anesthetized and the surgical area was sterilized. An incision was made over the lumbar spine, and a one- to two-level laminectomy was performed at the upper lumbar levels to access the spinal canal. A small incision was made in the dura, and an intrathecal catheter (EDM Lumbar Catheter; Medtronic, Minneapolis, MN) was inserted and advanced to the cervical cord under fluoroscopy. 0.5 mL of scAAV9-CB-IGF1 was then injected. The catheter was retracted 10 cm to the thoracic cord, and a second bolus of 0.5 mL was delivered. This was repeated for a third bolus delivered to the lumbar cord. The catheter was removed, and the dura was sutured in a running watertight manner. The muscle and skin were closed in layers.

Intraparenchymal vector delivery in the pig was performed as previously described.[12] Briefly, the animal was anesthetized and the surgical area was sterilized. A 22-cm incision was made through the skin and muscle overlying the cervical spine to expose the spinous processes and laminar surface. A three-layer laminectomy was performed at the C3–C5 levels to provide access to the spinal cord, and a 2.5-cm incision was made in the dura. The microinjection platform was mounted to the animal on the occiput and C7 spinous process. The pia was then opened. Ten pairs of bilateral injections were then made with a floating cannula: 2 mm medial relative to the dorsal root entry zone, 3.5 mm deep relative to the pial surface, with $\sim$2 mm between each injection. Twenty-five microliters of vector was injected at each site at a rate of 5 μL/min. Following infusion, the cannula was left in place for 5 min to minimize reflux. After all injections were complete, the dura was closed in a running watertight manner, and the muscle and skin were closed in layers.

Intrathecal vector delivery in the mouse was adapted from previous work.[13] Male B6SJL/J mice (Jackson Laboratories, Bar Harbor, ME) were anesthetized with isoflurane, and the depth of anesthesia was gauged by toe pinch. A rolled paper towel was placed under the lumbar spine to help separate the C5 and C6 lamina. An incision was made over the lower lumbar spine, and the spinous processes of C5 and C6 were identified. Ten microliters was loaded into a 27-gauge, 1 mL insulin syringe. The needle was inserted into the lumbar cistern by positioning the tip to one side of the C6 spinous process and angling the needle down and medially so that in slipped between the spinous process and the transverse process and under the C5 lamina. Proper position of the needle was assessed by the distance the needle was able to advance and the lack of reflux during the injection. In the case of reflux, the fluid was removed with a cotton swab and the injection was attempted a second time. The skin was then stapled shut with an Autoclip Applier (Stoelting, Wood Dale, IL), and the animal was placed on a warm pad during recovery.

Immunohistochemistry

At the time of euthanasia, rats were anesthetized with 5% isoflurane and euthanized with 100 mg/kg pentobarbital. Saline followed by 4% paraformaldehyde was delivered by cardiac perfusion. The spinal column was then removed and postfixed in 4% paraformaldehyde overnight. The spinal cord was removed and cryopreserved in 30% sucrose. Samples were embedded in Tissue-Tek® O.C.T. Compound (VWR, Radnor, PA) and sectioned at 40 μm on a Leica CM1950 cryostat (Wetzlar, Germany). Three weeks after vector delivery, pigs were perfused with saline, and spinal cord segments for immunohistochemistry (IHC) were harvested, fixed overnight in 4% paraformaldehyde, and cryopreserved in 30% ethylene glycol, 30% sucrose in 0.1 M phosphate buffer, pH 7.5, and sectioned on the cryostat.

A rabbit anti-green fluorescent protein (GFP) primary antibody (AB3080P; Millipore, Billerica, MA), biotinylated goat anti-rabbit secondary (111-065-144; Jackson ImmunoResearch, West Grove, PA), Vector ABC kit with HRP detection (PK-4000; Vector, Burlingame, CA), and Vector SG peroxidase substrate kit (SK-4700; Vector) were used to detect GFP expression. The primary was used at a 1:500 dilution and the secondary at 1:250. For IGF1 detection, a rabbit anti-IGF1 primary antibody (ab134140; Abcam, Cambridge, MA) was used at the same dilution and under the same conditions. For pig samples, sections were counterstained lightly with eosin. Images were collected with a Nikon (Tokyo, Japan) Eclipse E400 microscope with a Nikon Digital Sight controller and DS-Fi1 camera.

Vector titer

Vector preparations were titered by quantitative PCR (qPCR). Samples of each vector were serially diluted in 1×PCR buffer (10 mM Tris-HCl, pH 8.0, 50 mM KCl, 5 mM $MgCl_2$). One hundred microliters of each dilution was transferred to a new PCR tube and 1 μL of DNase I was added (Cat. No. 18047-019; Invitrogen, Waltham, MA). Nonencapsidated DNA was digested for 30 min at 37°C, and then, the DNase I was inactivated by incubation at 95°C for 10 min. To digest the capsid, 1 μL Proteinase K (Qiagen, Germantown, MD) was added to each sample, and the samples were incubated at 60°C for 1 h followed by 20 min at 95°C to inactivate the proteinase.

To create a standard curve, pTR-CB-GFP was digested with ScaI-HF in 1×CutSmart buffer (New England Biolabs) at 37°C for 1 h. The enzyme was inactivated by incubation at 80°C for 20 min. The digested plasmid was then serially diluted in 1×PCR buffer to create a standard curve. Two microliters of each standard and each virus sample were quantified using SYBR® Green JumpStart™ Taq ReadyMix™ (Sigma–Aldrich, St. Louis, MO) with primers against eGFP (forward primer: 5′-AAGGGCATCGACTTCAAGG-3′; reverse primer: 5′-TGCTTGTCGGCCATGATATAG-3′) on a 7500 Fast Real-Time PCR System (Applied Biosystems, Foster City, CA). Four dilutions of each vector ($1:10^2$ to $1:10^5$) were assayed in triplicate, and the values are reported as the average of these four dilutions.

Vector quantification in pig tissue

qPCR was performed by MPI Research (Mattawan, MI) to quantify vector levels in pig tissue. DNA was isolated using the QIAsymphony DSP DNA Mini Kit on a QIAsymphony instrument. DNA concentration was measured with a NanoDrop 8000 Spectrophotometer. A standard curve was generated using pTR-CB-IGF1 and prepared in the presence of 1,000 ng of pig liver DNA. qPCR was performed on an Applied Biosystems 7900HT Fast Real Time PCR System using TaqMan Universal Master Mix II (Thermo Fisher Scientific, Waltham, MA) and targeting the SV40 polyadenylation sequence (forward primer 5′-TGGT GGTGCAAATCAAAGAACT-3′; reverse primer: 5′-AACACTTCCGTACAGGCCTAGAA-3′; probe: 5′-6FAM-CTCAGTGGATGTTGCCTT-MGB-3′). The data were initially recorded as vector copies per 1,000 ng of DNA for tissue, per 100 ng of DNA for blood, or per 10 μL of CSF. Vector copies for tissue and blood were converted to vector copies per diploid genome assuming a genome size of 5.4×10^9 base pairs and an average molecular weight of 650 Da per base pair.

Measurement of transduction *in vitro*

NSC-34 and HEK293 cells were maintained in Dulbecco's modified Eagle medium (D5796; Sigma–Aldrich) supplemented with 10% fetal bovine serum and 0.1% penicillin–streptomycin (#15070-063; Thermo Fisher Scientific) and split at 80–90% confluence. Twenty-four hours before transduction, the cells were plated in 48-well plates at a density of 1.4×10^4 cells per well. Cells were transduced in triplicate at two multiplicities of infection (MOIs): 2.5×10^5 and 2.5×10^4, making the assumption that the cells divided once in the 24 h between plating and transduction. Untreated cells served as a negative control. Due to autofluorescence in the media, the media was replaced with phosphate-buffered saline immediately before imaging. For each well, two nonoverlapping regions were imaged at random. For each region, two images were obtained on a Leica DM IRE2 inverted microscope (Buffalo Grove, IL): one under brightfield and one using fluorescence. The exposure time for fluorescence was empirically determined so that no cells bodies were detected in the negative control wells. For HEK293 cells, the fluorescence and brightfield images were processed through ImageJ to measure the area occupied by the transduced cells and all cells, respectively, and the results were reported as the percentage of the area occupied by the cells that were GFP positive. Due to the larger variation in cell diameter observed in NSC-34 cultures, cells were counted manually and expressed as the percentage of cells that were GFP positive. For both cell types, the results are presented as the average ± the standard deviation of three wells.

Sodium dodecyl sulfate–polyacrylamide gel electrophoresis and silver stain

For six scAAV9 lots, 1.5×10^{10} vector genomes (vg) of virus in 5 μL were mixed with 5 μL 2×Laemmli buffer (#1610737; Bio-Rad, Hercules, CA), prepared according to the manufacturer's instructions. The samples were heated to 95°C for 5 min and then cooled to room temperature. The samples were loaded onto a 4–15% Mini-PROTEAN TGX Stain-Free Gel (#4568086; Bio-Rad) and run at 90 V for 90 min. The gel was then removed from the plastic cassette and stained with a Pierce Sliver Stain Kit (#24612; Thermo Fisher Scientific) according to the manufacturer's instructions. The gel was transferred to a smooth, white background and photographed with an Apple iPhone 6.

RESULTS

Gray matter transduction by scAAV9-CB-GFP

Since intrathecal delivery of scAAV9 had not previously been reported in rats, a pilot study was conducted. A self-complimentary AAV9 vector expressing GFP from a CMV enhancer and chicken β-actin promoter (scAAV9-CB-GFP) was obtained from Core A (lot 1, Table 1). This vector was injected intrathecally (IT) via a catheter threaded from the CM to the lumbar level of the spinal cord into male Sprague-Dawley rats. The animals were euthanized 3 weeks later and perfused. Gray matter transduction was observed along the length of the cord (Fig. 1A, B), consistent with previous reports in other animal models.

Based on these pilot data, two new lots were obtained from Core A, a therapeutic vector, and a new lot of scAAV9-CB-GFP to serve as a negative control (lot 2). A therapeutic study was initiated that included nine animals receiving scAAV9-CB-GFP. As the animals reached endpoint, the spinal cords were harvested and stained for GFP. In contrast to the pilot, no gray matter transduction was observed in any of the scAAV9-CB-GFP-treated animals (Fig. 1C, D). Dorsal root ganglia (DRGs) and white matter tracks stained positive for GFP, demonstrating that the vector was infectious. Since these animals were harvested later than the pilot animals, a third lot of scAAV9-CB-GFP was obtained from Core A (lot 3). The new lot was injected as above, and the animals were harvested at 3 weeks. Again, no transduction of the gray matter was observed ($n=4$; Table 1). However, unilateral injection of the vector into the gray matter yielded robust transduction (Fig. 1E), demonstrating that the vector could transduce the gray matter if delivered directly.

To determine if this problem was specific to Core A, new scAAV9-CB-GFP preparations were obtained from Core B (lot 4) and Core C (lot 5). These vectors were injected IT ($n=3$ per preparation), and the animals were harvested after 3 weeks. Only lot 4 produced detectable staining in the gray matter (Table 1). These results suggested that the problem was not core-specific.

Transduction by other scAAV9 vectors

To determine if the variation between lots was a problem specific to the scAAV9-CB-GFP genome, several different GFP-expressing scAAV9 vectors were obtained from four vector cores and tested in Sprague-Dawley rats as described above (lots 7–10). In addition, an older lot of scAAV9-miniCAG-GFP was also tested (lot 6). Only one of these preparations, the older lot of scAAV9-miniCAG-GFP transduced the gray matter (Table 1). These results suggest that the problem encountered with intrathecal delivery of scAAV9 is neither core- nor vector genome-specific. In addition, animals from the same colony of Sprague-Dawley rats housed under

Table 1. *Research grade scAAV9 lots used in this study*

Lot no.	*1 (pilot)*	*2*	*3*	*4*	*5*	*6*	*7*	*8*	*9*	10
Source	Core A	Core A	Core A	Core B	Core C	Core D	Core D	Core E	Core C	Core F
Vector	CB-GFP	CB-GFP	CB-GFP	CB-GFP	CB-GFP	miniCAG-GFP	miniCAG-GFP	CMV-GFP	CBA-GFP	scCB6-PI-GFP
Gray matter transduction	+	–	–	+	–	+	–	–	–	–
Purification	CsCl	Iodixinol/Chrom.	Iodixinol/Chrom.	CsCl	Iodixinol/Chrom.	CsCl	CsCl	Iodixinol/Chrom.	Iodixinol/Chrom.	Iodoxinol
Buffer	A	A	A	B	C	D	D	E	C	F
Core titer (vg/mL)	5.7×10^{12}	4.2×10^{12}	8.3×10^{12}	1.7×10^{13}	1.7×10^{12}	1.2×10^{13}	1.5×10^{13}	1.4×10^{13}	4.0×10^{12}	3.4×10^{12}
Retitered (vg/mL)	ND	ND	2.5×10^{12}	3.0×10^{13}	ND	2.4×10^{13}	5.2×10^{13}	1.1×10^{13}	6.4×10^{12}	1.5×10^{13}

A: 20 mM Tris, pH 8.0, 1 mM $MgCl_2$, 200 mM NaCl, 0.001% Pluronic F68.
B: PBS with 0.001% Pluronic F68.
C: 350 mM NaCl, 5% sorbitol in PBS.
D: PBS with 5% sorbitol and 0.001% Pluronic F68.
E: Lactated ringers.
F: PBS with additional 35 mM NaCl, 5% glycerol.
CBA, chicken β-actin promoter; CMV, cytomegalovirus promoter; ND, not done; PBS, phosphate-buffered saline; vg, vector genomes.

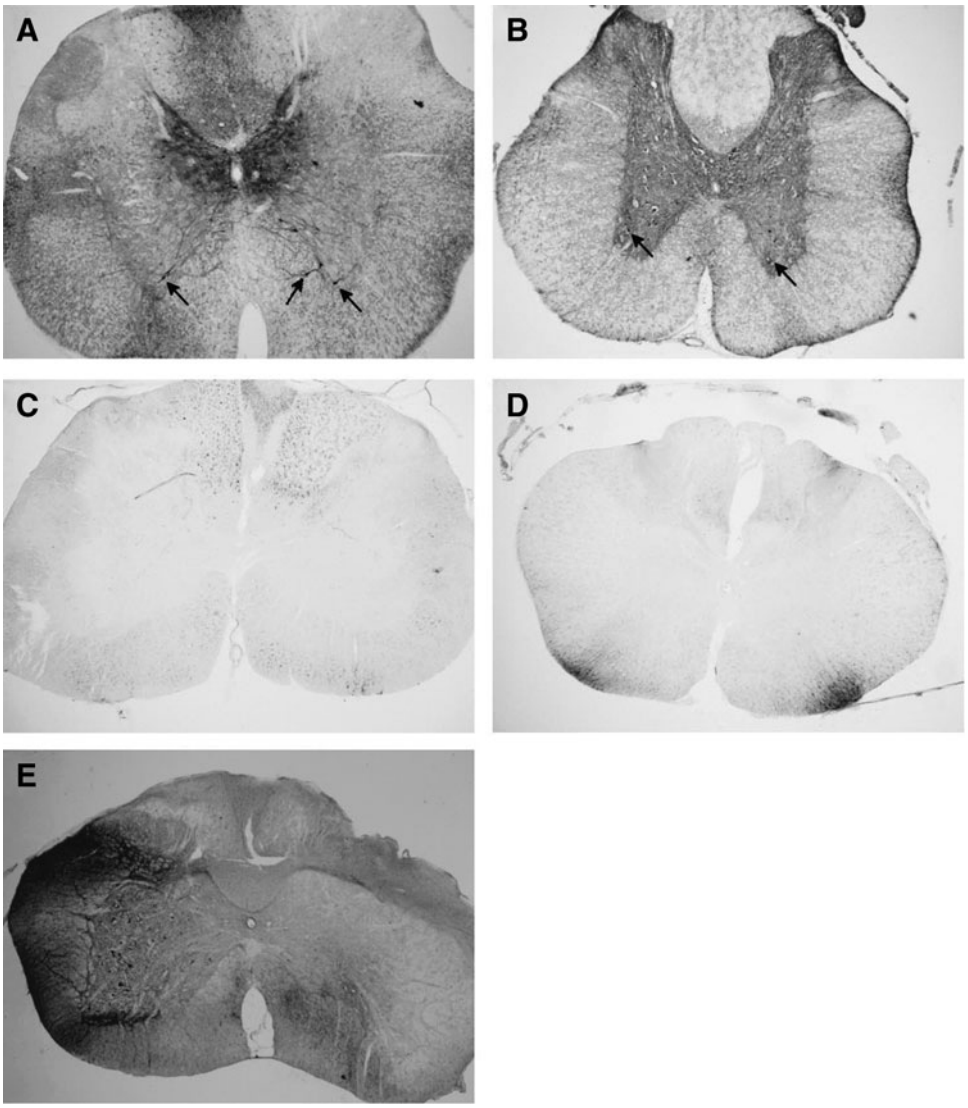

Figure 1. Gray matter transduction following intrathecal scAAV9 delivery. Seventy-day-old Sprague-Dawley rats received a 30 μL intrathecal injection of scAAV9-CB-GFP via an intrathecal catheter, threaded from the cisterna magna down to lumbar level of the spinal cord. Three weeks later, the spinal cords were harvested, sectioned, and stained for GFP (*black stain*). **(A)** Cervical and **(B)** lumbar spinal cord sections from animals that received the pilot lot from Core A are shown. At all levels of the spinal cord, robust transduction was observed in the gray matter, including cells morphologically similar to motor neurons (*arrows*). **(C)** Cervical and **(D)** lumbar spinal cord sections from animals receiving lot 2 from Core A are shown. In contrast to the animals in **(A, B)**, no gray matter transduction was observed. White matter tracts did stain positively for GFP, possibly due to DRG transduction. **(E)** When directly injected unilaterally into the spinal cord, a nonpenetrating vector yielded robust transduction of the gray matter on the treated side (*left*). DRG, dorsal root ganglia; GFP, green fluorescent protein; scAAV9, self-complementary adeno-associated virus serotype 9.

the same conditions were used to test all lots of vector, ruling out differences in animal strain or environment.

Lot parameters do not correlate with transduction

We next considered three other potential sources of variability: production scheme, buffer, and titer. The lots tested thus far had either been purified on a continuous CsCl gradient or by iodixinol gradient with or without affinity chromatography purification. Core A had moved away from CsCl banding between the first lot that did transduce the gray matter and those that did not, and the second penetrating lot had also been purified on a CsCl gradient. However, there was no consistent relationship of purification scheme with gray matter transduction (Table 1). The vectors were dialyzed against a variety of buffers, but there was no obvious correlation between buffer and transduction.

Errors in vector titering were also considered given previous reports regarding difficulties in quantifying AAV preparations by qPCR.[14] Seven lots for which we had sufficient material left were

retitered head-to-head using primers against the GFP cDNA, which was common among all the vectors. The titers measured by our assay were comparable to the titers provided by the cores that produced these lots, with no more than a 4.5-fold variance between the two measurements (Table 1). In addition, there was no correlation between vector titer and gray matter transduction.

Whole-particle mass spectrometry

We next considered the possibility that there were gross structural differences between penetrating lots and nonpenetrating lots. Two lots of scAAV9-CB-GFP were evaluated by charge detection mass spectrometry (CDMS)[15]: a nonpenetrating lot from Core C (lot 5) and a penetrating lot from Core B (lot 4). Both lots produced a dominant peak with a weight that correlated with the mass expected for a particle carrying half of a genome (partial) and a peak corresponding to a full-length genome (Fig. 2). In addition, the nonpenetrating lot (Fig. 2B) contained a small peak of empty capsids as well as some high– and low–molecular weight peaks of unknown identity. Neither of these features was prominent in the penetrating lot (Fig. 2A). Empty capsids have been shown to inhibit transduction,[16] but not at the low levels found in this lot. The implications of the high– and low–molecular weight impurities are unclear.

Good Laboratory Practice lot evaluated in pigs

A Good Laboratory Practice (GLP) lot of scAAV9-CB-IGF1 was produced at Core C as part of a rapid development program for efficacy, biodistribution, and toxicology studies. It was expected that the GLP lot would be immune to the problem observed in the majority of research-grade preparations. In consultation with the head of the vector core, a number of quality control criteria were chosen ahead of production. This lot met all the release criteria (Supplementary Table S1).

A pilot experiment was carried out in Göttingen minipigs. Two pigs received intrathecal scAAV9-CB-IGF1 as performed previously,[10] and two received 20 intraparenchymal injections into the cervical spinal cord targeting the ventral horns. Three weeks after vector delivery, the animals were euthanized and tissue was taken for IHC, qPCR, and pathology.

qPCR results are shown in Fig. 3. For the two animals receiving intraparenchymal injections, the highest quantity of vector genomes was found at the site of the injections, reaching ~100 copies per diploid genome. Transduction of the gray matter in spinal cord regions distant from the injections was substantially lower, ~0.1% of the level in the cervical cord, suggesting that the vector did not spread far from the injection site. Low levels of vector genomes were also found in peripheral tissues. Strikingly, animals that received intrathecal

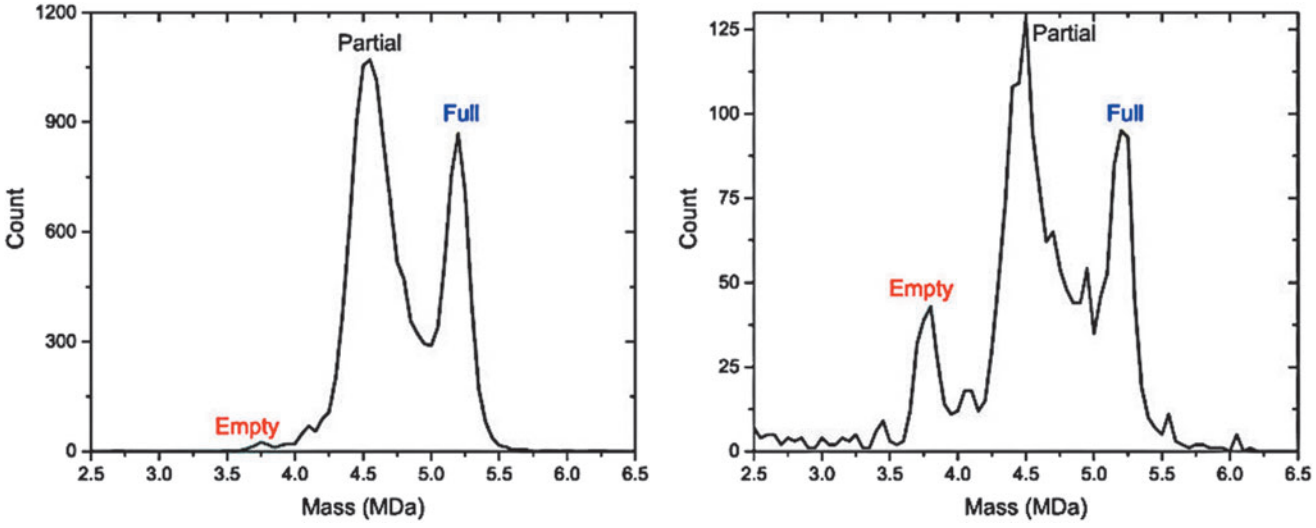

Figure 2. Mass spectrometry reveals differences in scAAV9 preparations. Charge detection mass spectrometry was used to characterize two scAAV9-CB-GFP lots: one penetrating lot (lot 4, **A**) and one nonpenetrating lot (lot 5, **B**). Peaks with masses predicted for filled, partially filled, and empty capsids are identified. The predominant band in both lots has a mass similar to the predicted molecular weight for a capsid packaging half of a genome, comprising 61% of the area under the curve in lot 4 and 51% in lot 5. Particles containing a full-length genome represented 27% and 23% of the area for these two lots, respectively. In addition, the nonpenetrating lot has a peak corresponding to empty capsids representing 9% of the area as well as a collection of high–molecular weight material of unknown identity.

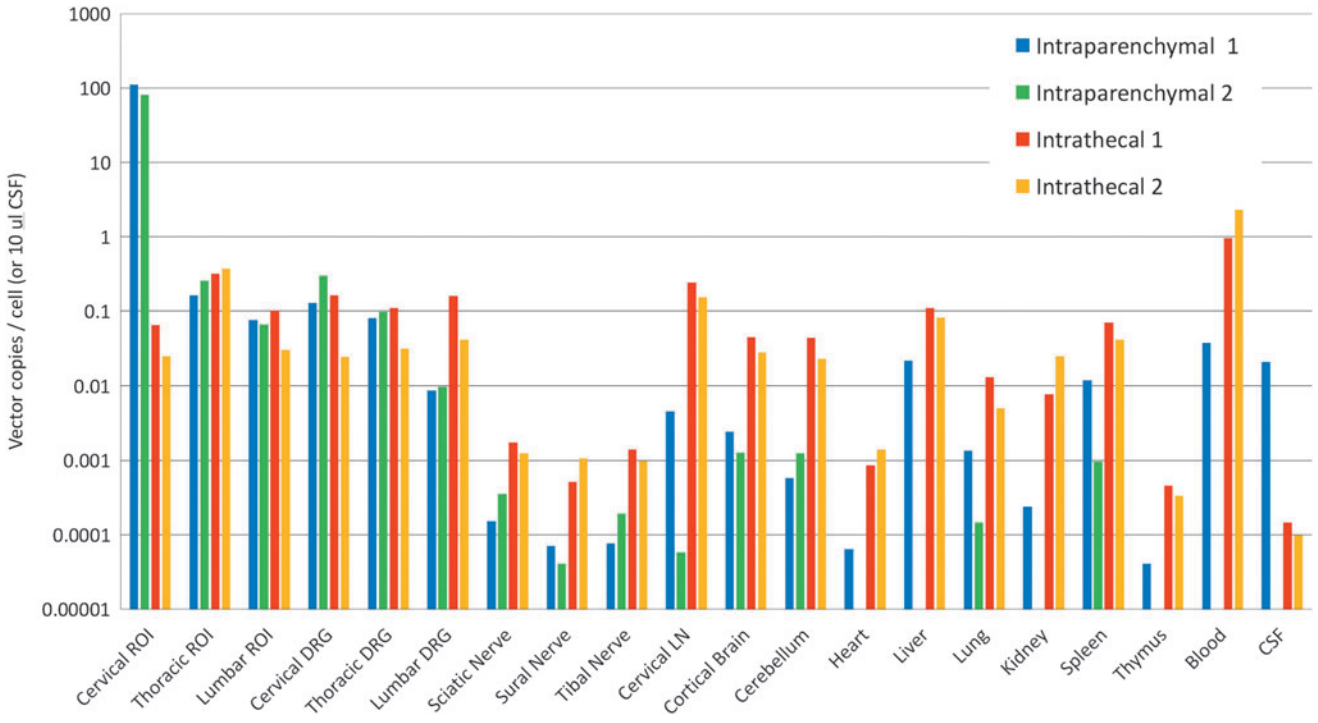

Figure 3. scAAV9-CB-IGF1 biodistribution in pigs. A GLP lot of scAAV9-CB-IGF1 was injected intraparenchymally into the cervical cord of two pigs (20 injections, 2.5×10^{11} vg/inj.) or IT via a catheter (500 μL per spinal cord region [cervical, thoracic, and lumbar], 1.4×10^{13} vg/mL) in two pigs. Three weeks later, the animals were euthanized and tissues were collected. Quantitative PCR was performed on the brain, spinal cord, and peripheral tissues to measure vector genomes. Missing bars indicate samples where the vector copy number was below the limit of detection. The highest levels of transduction were observed in the cervical cord of pigs receiving parenchymal injections. IT delivery did not result in greater transduction in the thoracic and lumbar cord compared with pigs receiving cervical injections, even though the total dose was nearly sixfold higher. CSF, cerebrospinal fluid; GLP, Good Laboratory Practice; IT, intrathecally; LN, lymph node; ROI, region of interest; vg, vector genomes.

scAAV9 delivery achieved vector copies in the spinal cord similar to those of the uninjected regions of animals receiving parenchymal injections, suggesting that the vector failed to reach the gray matter. Relative to the pigs receiving intraparenchymal injections, IT delivery led to greater numbers of genomes in the brain, DRGs, nerves, and peripheral tissues (Fig. 3).

Spinal cord sections from both cohorts were stained for IGF1. Consistent with the qPCR data, IGF1 expression was detected in the cervical cords of animals receiving intraparenchymal injections (Fig. 4). No positive staining could be detected outside this region in pigs receiving intraparenchymal scAAV9 or in any spinal cord region in animals receiving IT scAAV9. These data again suggest that the GLP lot is nonpenetrating. These results indicate that GLP lots are not immune to the problem observed with research-grade vectors.

The GLP lot does not inhibit a penetrating lot

One potential hypothesis to explain the above data is that nonpenetrating lots contain soluble inhibitory factors that prevent the virus particles from reaching the gray matter. To test this model, scAAV9-CB-GFP from lot 4 was diluted 1:10 into the GLP scAAV9-CB-IGF1 preparation and injected IT into mice ($n=6$). As a positive control, scAAV9-CB-GFP was injected neat into a second cohort ($n=4$). Similar to rats receiving an IT injection of the penetrating lot, scAAV9-CB-GFP-treated mice showed robust transduction in the gray matter along the length of the cord (Fig. 5). IGF1-GFP-treated mice also exhibited gray matter transduction along the length of the cord. Staining was reduced relative to scAAV9-CB-GFP-treated mice but appeared to be consistent with the 1/10th dose that was delivered to these animals. This result suggests that a nonpenetrating lot does not contain soluble factors that inhibit transduction.

In vitro analysis of transduction

Five scAAV9 lots expressing GFP were assayed *in vitro* for their ability to transduce neuronal-lineage cell types, two penetrating lots and three nonpenetrating lots. NSC-34 and HEK293 cells were transduced at MOIs of 2.5×10^5 and 2.5×10^4. Forty-eight hours after transduction, the trans-

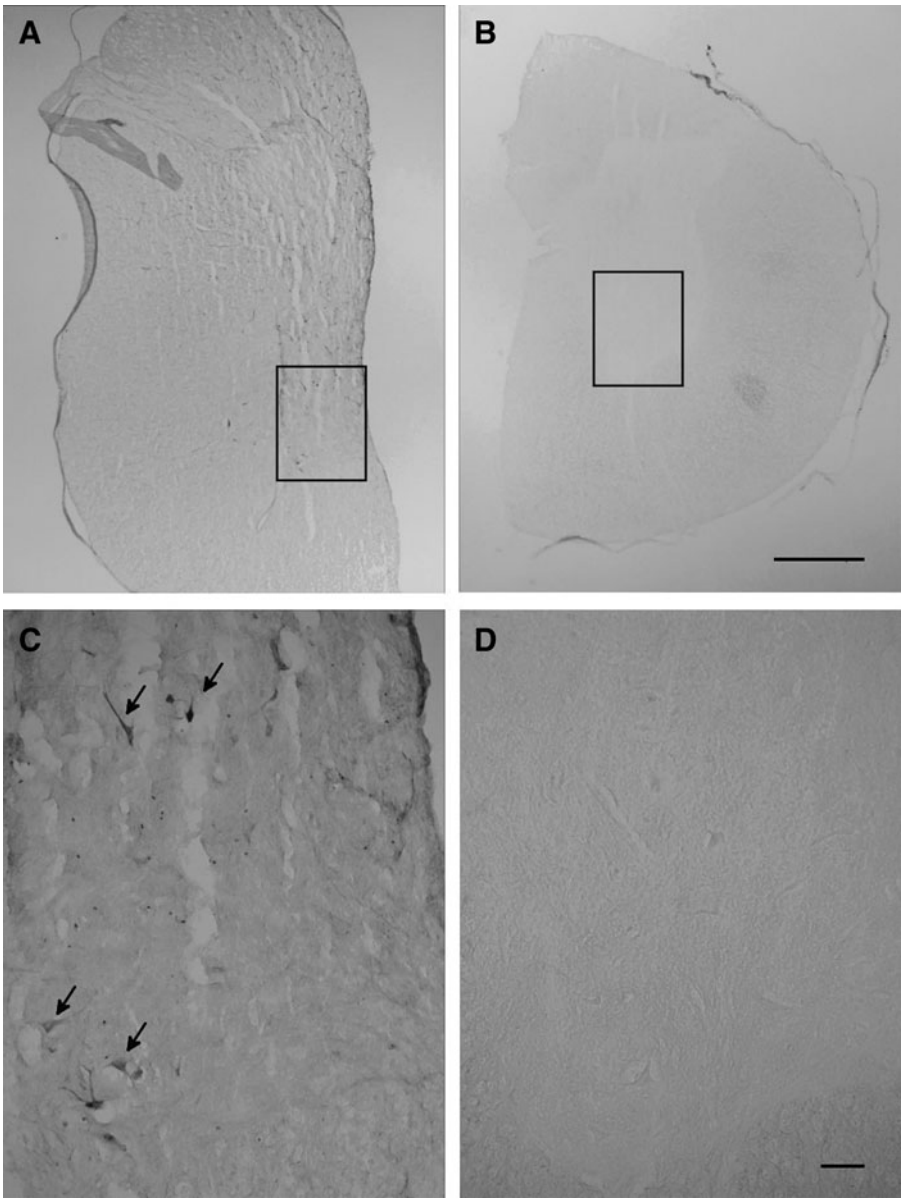

Figure 4. IGF1 expression in pig spinal cord. scAAV9-CB-IGF1 was injected intraparenchymally into the cervical cord of two pigs (20 injections, 2.5×10^{11} vg/inj.) or IT via a catheter threaded from the lumbar spine (500 μL per spinal cord region [cervical, thoracic, and lumbar], 1.4×10^{13} vg/mL). Three weeks later, the animals were euthanized and tissues were collected. **(A)** In pigs receiving parenchymal injections, IGF1 was detected in the cervical cord (*black stain*) but not in other regions. Some positive cell bodies are apparent and the entire gray matter is faintly stained as expected for a secreted protein. **(B)** In contrast, animals receiving intrathecal injections showed no evidence of IGF1 expression at any spinal cord level. A section from the lumbar cord is shown. **(C, D)** The ventral areas indicated by the boxes in **(A, B)**, respectively, are shown at higher magnification. *Arrows* indicate IGF1-positive cells with large somas that are likely motor neurons. The scale bar for **(A, B)** represents 1 mm and the scale bar for **(C, D)** represents 100 μm. IGF1, insulin-like growth factor 1.

duction efficiency at each MOI was determined. The results of the higher MOI are shown (Fig. 6A, B). Similar results were observed in the HEK293 cells at the lower MOI (data not shown). In NSC-34 cells, little transduction was observed in all the samples at the lower MOI, so those samples were not quantified. Differences in transduction were observed between all the lots. The non-penetrating lots yielded less transduction than the penetrating lots. In one case, lot 7, transduction was reduced 21-fold relative to lot 4. Transduction by lots 8 and 10 was approximately two- to threefold lower than lot 4.

Polyacrylamide gel electrophoresis/silver stain analysis of vectors

The five scAAV9 lots expressing GFP assayed above and the GLP scAAV9-IGF1 lot were analyzed by sodium dodecyl sulfate–polyacrylamide gel electrophoresis (SDS-PAGE) followed by silver stain to

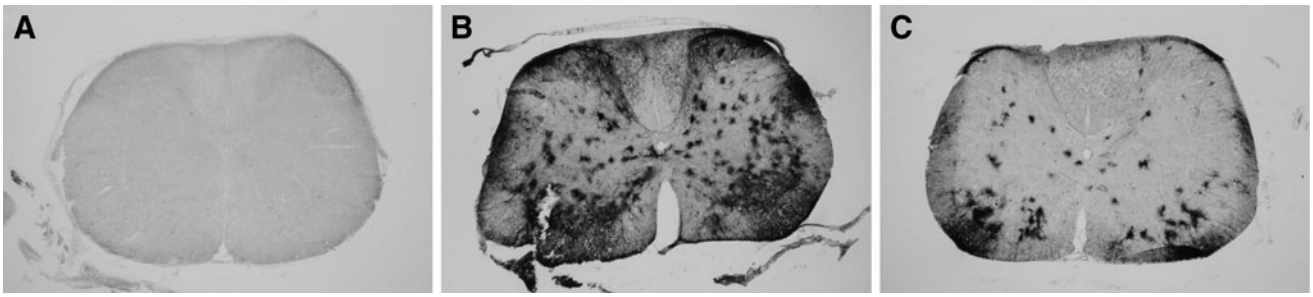

Figure 5. A nonpenetrating scAAV9 lot does not inhibit a penetrating lot. Seventy-day-old mice received an intrathecal injection of scAAV9-CB-GFP (10 μL at 1.7×10^{13} vg/mL; lot 4) or the GLP scAAV9-CB-IGF1 (10 μL at 1.4×10^{13} vg/mL) spiked with a 1:10 volume of the GFP vector (IGF1-GFP-treated). Approximately 70 days later, the animals were euthanized and the spinal cords were sectioned and stained for GFP. Shown are representative sections of cervical spinal cord from **(A)** untreated, **(B)** scAAV9-CB-GFP-treated, and **(C)** IGF1-GFP-treated mice. IT delivery of the GFP vector resulted in robust transduction of the spinal cord (*black stain*). Mixing a 1:10 volume of this preparation into the GLP preparation did not inhibit the ability of the GFP vector to transduce the gray matter.

look for the presence of contaminants that might explain the differences in transduction efficiency *in vivo*. 1.5×10^{10} vg were analyzed in each lane. Three bands dominated in all the lots, likely corresponding to VP1, VP2, and VP3. Although each lane contained the same amount of vector genome, there was substantial variation in the amount of the capsid proteins. No two lots exhibited the same pattern of contaminants.

DISCUSSION

Reproducibility is a hallmark of science. Ideally, two laboratories evaluating the same viral vector and delivery approach will observe the same biodistribution *in vivo*. However, as the literature suggests and our data have shown, obtaining reproducible results with intrathecal scAAV9 vectors can be a significant challenge. In the current study, two surgeons performed all the surgeries. Each surgeon injected half of the animals for each vector. Both surgeons obtained identical results for each vector, suggesting that individual technique is not a factor in the observed lot-to-lot variation.

The source of the observed variation in transduction is unclear. The problem is not specific to one vector core or one particular vector genome. Two of the six cores used produced both penetrating and nonpenetrating lots of the same vector. The problem also does not appear to be species specific since it manifested in both rats and pigs. CsCl-purified AAV vectors can contain contaminants that inhibit transduction.[17,18] However, all the penetrating vectors identified in this study were purified on CsCl gradients.

Other potential sources of lot-to-lot variation include osmolarity, the presence of endotoxins, aggregation of virus particles, the presence of empty capsids,[16,19,20] an immune response against the vector, action by residual CsCl, the integrity of the vector genome, and other protein contaminants.[21–23] Lim-

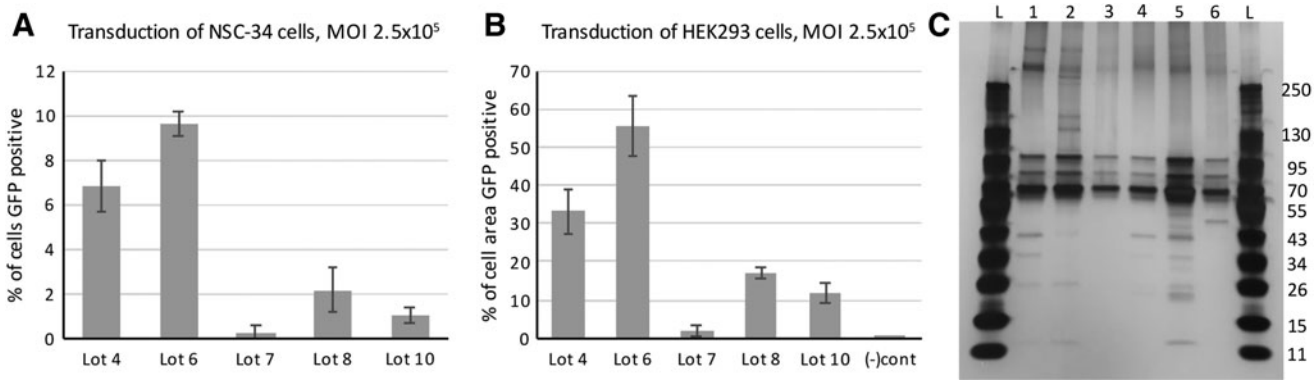

Figure 6. *In vitro* characterization of scAAV9 lots. **(A)** NSC-34 cells and **(B)** HEK293 cells were infected with two penetrating lots (lots 4 and 6) and three nonpenetrating lots (lots 7, 8, and 10) of scAAV9 expressing GFP at an MOI of 2.5×10^5. Forty-eight hours after infection, the cells were imaged under fluorescent microscopy and light microscopy to determine the fraction of cells transduced. **(C)** 1.5×10^{10} vg of vector were analyzed using SDS-PAGE and silver stain. Lanes: L, ladder (weights given in kDa on *right*); 1, lot 4; 2, lot 6; 3, lot 7; 4, lot 8; 5, lot 10; 6, GLP lot. In all lots, the three bands corresponding to VP1, VP2, and VP3 (87, 73, and 62 kDa, respectively) are the dominant species. Contaminants of unknown identity are present in all lots and vary from lot to lot. Although equal numbers of vector genomes were loaded, the total mass of capsid proteins varied between lots. MOI, multiplicity of infection; SDS-PAGE, sodium dodecyl sulfate–polyacrylamide gel electrophoresis.

ited quantities of the vectors precluded us from measuring osmolarity, endotoxins, CsCl concentration, immune response, and aggregation in the research-grade lots. However, the mixing experiment where a small amount of a penetrating vector spiked into a nonpenetrating vector showed that transduction of the penetrating vector is not inhibited. This observation suggests that osmolarity, endotoxins, and CsCl concentration do not likely underlie the lot-to-lot variation in gray matter transduction. Notably, these types of assays are not commonly used by researchers performing *in vivo* studies of research-grade vectors. Given our results, although, these are assays one should consider at the outset of any study involving viral vectors.

For five scAAV9 lots expressing GFP (two penetrating and three nonpenetrating) for which samples remained after the *in vivo* experiments, *in vitro* transduction and PAGE were performed. Silver stain of the samples did not reveal any differences between the penetrating and nonpenetrating vectors. One nonpenetrating lot did show a 21-fold reduction in transduction of NSC-34 and HEK293 cells, lines that have some neuronal characteristics. However, the other two nonpenetrating lots showed only mildly reduced potencies, differences not consistent with the complete lack of gray matter transduction observed *in vivo*. Whether this reflects a lower overall infectivity of these vectors or a difference in their affinity for these cell types is unknown. CDMS analysis of one nonpenetrating lot revealed high–molecular weight impurities in this preparation. Unknown are the identities of these impurities and whether they appear in all nonpenetrating lots.

The mixing experiment conducted in mice suggests that the problem in the nonpenetrating lots is not a soluble factor. This could point to differences in capsid composition or to modifications of the surface of the capsid. Capsid composition is known to vary from lot-to-lot. The relative ratio of VP1:VP2:VP3 is often quoted as 1:1:10. However, we were unable to identify a primary source for this ratio. The earliest estimate in the literature, ~1:1:20, was reported by Rose *et al.* for AAV serotypes 1, 2, and 3.[24] The estimate of 1:1:10 is sometimes directly or indirectly misattributed to this article. Shortly thereafter, Johnson *et al.* reported a ratio of ~1:1:8 for AAV3.[25] Variation in capsid composition has been reported in the intervening years, ranging from 1:1:5 to 1:1:20,[26] possibly dependent on the cell line used to manufacture the vectors.[27] This variation can affect transduction efficiency and the transduction profile.[27] In addition, these bulk measurements of capsid protein stoichiometry belie particle-to-particle variability within a single preparation.[28] Identifying new ways to interrogate the structures of individual capsids may help shed light onto the mechanisms underlying lot-to-lot variation in AAV preparations.

How AAV9 vectors reach the gray matter from the CSF space is currently unclear. To reach the gray matter from the CSF, the vector presumably must cross both the pia mater and the glia limitans. The pia mater is fenestrated in the Virchow-Robin spaces (VRS),[29] possibly providing a direct path for AAV9 through this barrier. Consistent with this idea, it has been suggested that intrathecal AAVrh10 enters the interior of the spinal cord, in part, by passing through the VRS.[30]

The glia limitans is composed of astrocytic end feet connected by tight junctions, likely representing the greatest barrier between the gray matter and the intrathecal space. Interestingly, there are also astrocytic end feet associated with the blood–brain barrier. Studies of intravenous delivery of scAAV9 have yielded different patterns of transduction, with some observing primarily astrocyte transduction. It is tempting to speculate that these studies used lots similar to our nonpenetrating preparations and that the virus particles fail to cross the astrocytic end feet, resulting in little neuronal transduction. If true, the problem that we have described may have implications for other routes of scAAV9 delivery.

While some inconsistencies might be expected from research-grade lots, which undergo less stringent quality control testing, the problem with the GLP lot was surprising. This lot underwent substantial release testing that was developed in concert with the director of the core. At an increasing rate, gene therapy vectors are moving into clinical trials and receiving approvals, including those for intrathecal delivery of AAV9 vectors.[31] The failure of the GLP vector raises the pressing question about how to ensure consist potency between lots. Measures of impurities, such as residual cell proteins and empty capsids, were not sufficient in this case to predict a problem with the vector. Clearly, other assays are needed. Animal testing is one possible option, although genetic drift in animal colonies occurring over years or decades may make this approach less than reliable in the long term.[32–34] Identifying the underlying problem would allow for the development of *in vitro* assays to screen new lots. Better tools to characterize vector composition and a better understanding of how variation in composition affects transduction are needed.

ACKNOWLEDGMENTS

We wish to thank Mark Potter, Guangping Gao, Andrew Moreo, Adam Davis, and Shangzhen Zhou

for their helpful discussions about this project. The GLP vector was provided by Above and Beyond, LLC.

AUTHOR DISCLOSURE

A.D. is an inventor on a patent regarding the use of AAV9 vectors in the central nervous system.

FUNDING INFORMATION

This work was supported by National Institutes of Health (NIH) grant 1R21NS085553.

SUPPLEMENTARY MATERIAL

Supplementary Table S1

REFERENCES

1. Foust KD, Nurre E, Montgomery CL, et al. Intravascular AAV9 preferentially targets neonatal neurons and adult astrocytes. Nat Biotechnol 2009;27:59–65.
2. Gray SJ, Matagne V, Bachaboina L, et al. Preclinical differences of intravascular AAV9 delivery to neurons and glia: a comparative study of adult mice and nonhuman primates. Mol Ther 2011;19: 1058–1069.
3. Donsante A, McEachin Z, Riley J, et al. Intracerebroventricular delivery of self-complementary adeno-associated virus serotype 9 to the adult rat brain. Gene Ther 2016;23:401–407.
4. Goenawan H, Hirai H. Modulation of lentiviral vector tropism in cerebellar Purkinje cells in vivo by a lysosomal cysteine protease cathepsin K. J Neurovirol 2012;18:521–531.
5. Schuster DJ, Dykstra JA, Riedl MS, et al. Biodistribution of adeno-associated virus serotype 9 (AAV9) vector after intrathecal and intravenous delivery in mouse. Front Neuroanat 2014;8:42.
6. Bucher T, Dubreil L, Colle MA, et al. Intracisternal delivery of AAV9 results in oligodendrocyte and motor neuron transduction in the whole central nervous system of cats. Gene Ther 2014;21:522–528.
7. Haurigot V, Marco S, Ribera A, et al. Whole body correction of mucopolysaccharidosis IIIA by intracerebrospinal fluid gene therapy. J Clin Invest 2013 [Epub ahead of print]; DOI: 10.1172/JCI66778.
8. Bevan AK, Duque S, Foust KD, et al. Systemic gene delivery in large species for targeting spinal cord, brain, and peripheral tissues for pediatric disorders. Mol Ther 2011;19:1971–1980.
9. Samaranch L, Salegio EA, San Sebastian W, et al. Strong cortical and spinal cord transduction after AAV7 and AAV9 delivery into the cerebrospinal fluid of nonhuman primates. Hum Gene Ther 2013; 24:526–532.
10. Federici T, Taub JS, Baum GR, et al. Robust spinal motor neuron transduction following intrathecal delivery of AAV9 in pigs. Gene Ther 2012;19:852–859.
11. De la Calle JL, Paino CL. A procedure for direct lumbar puncture in rats. Brain Res Bull 2002;59:245–250.
12. Federici T, Riley J, Park J, et al. Preclinical safety validation of a stabilized viral vector direct injection approach to the cervical spinal cord. Clin Transl Sci 2009;2:165–167.
13. Hylden JL, Wilcox GL. Intrathecal morphine in mice: a new technique. Eur J Pharmacol 1980;67: 313–316.
14. Fagone P, Wright JF, Nathwani AC, et al. Systemic errors in quantitative polymerase chain reaction titration of self-complementary adeno-associated viral vectors and improved alternative methods. Hum Gene Ther Methods 2012;23:1–7.
15. Pierson EE, Keifer DZ, Asokan A, et al. Resolving adeno-associated viral particle diversity with charge detection mass spectrometry. Anal Chem 2016;88:6718–6725.
16. Gao K, Li M, Zhong L, et al. Empty virions in AAV8 vector preparations reduce transduction efficiency and may cause total viral particle dose-limiting side-effects. Mol Ther Methods Clin Dev 2014;1: 20139.
17. Klein RL, Dayton RD, Tatom JB, et al. AAV8, 9, Rh10, Rh43 vector gene transfer in the rat brain: effects of serotype, promoter and purification method. Mol Ther 2008;16:89–96.
18. Ayuso E, Mingozzi F, Montane J, et al. High AAV vector purity results in serotype- and tissue-independent enhancement of transduction efficiency. Gene Ther 2010;17:503–510.
19. Sommer JM, Smith PH, Parthasarathy S, et al. Quantification of adeno-associated virus particles and empty capsids by optical density measurement. Mol Ther 2003;7:122–128.
20. Wright JF. AAV empty capsids: for better or for worse? Mol Ther 2014;22:1–2.
21. Tenenbaum L, Hamdane M, Pouzet M, et al. Cellular contaminants of adeno-associated virus vector stocks can enhance transduction. Gene Ther 1999;6:1045–1053.
22. Strobel B, Miller FD, Rist W, et al. Comparative analysis of cesium chloride- and iodixanol-based purification of recombinant adeno-associated viral vectors for preclinical applications. Hum Gene Ther Methods 2015;26:147–157.
23. Wright JF. Product-related impurities in clinical-grade recombinant AAV vectors: characterization and risk assessment. Biomedicines 2014;2:80–97.
24. Rose JA, Maizel JV, Jr., Inman JK, et al. Structural proteins of adenovirus-associated viruses. J Virol 1971;8:766–770.
25. Johnson FB, Ozer HL, Hoggan MD. Structural proteins of adenovirus-associated virus type 3. J Virol 1971;8:860–863.
26. Aucoin MG, Perrier M, Kamen AA. Critical assessment of current adeno-associated viral vector production and quantification methods. Biotechnol Adv 2008;26:73–88.
27. Kondratov O, Marsic D, Crosson SM, et al. Direct head-to-head evaluation of recombinant adeno-associated viral vectors manufactured in human versus insect cells. Mol Ther 2017;25: 2661–2675.
28. Snijder J, van de Waterbeemd M, Damoc E, et al. Defining the stoichiometry and cargo load of viral and bacterial nanoparticles by Orbitrap mass spectrometry. J Am Chem Soc 2014;136:7295–7299.
29. Zhang ET, Inman CB, Weller RO. Interrelationships of the pia mater and the perivascular (Virchow-Robin) spaces in the human cerebrum. J Anat 1990;170:111–123.
30. Guo Y, Wang D, Qiao T, et al. A single injection of recombinant adeno-associated virus into the lumbar cistern delivers transgene expression throughout the whole spinal cord. Mol Neurobiol 2016;53:3235–3248.
31. Bailey RM, Armao D, Nagabhushan Kalburgi S, et al. Development of intrathecal AAV9 gene therapy for giant axonal neuropathy. Mol Ther Methods Clin Dev 2018;9:160–171.
32. Stevens JC, Banks GT, Festing MF, et al. Quiet mutations in inbred strains of mice. Trends Mol Med 2007;13:512–519.
33. Farkas B, Boldizsar F, Tarjanyi O, et al. BALB/c mice genetically susceptible to proteoglycan-induced arthritis and spondylitis show colony-dependent differences in disease penetrance. Arthritis Res Ther 2009; 11:R21.
34. Simecek P, Churchill GA, Yang H, et al. Genetic analysis of substrain divergence in non-obese diabetic (NOD) mice. G3 (Bethesda) 2015;5:771–775.

Received for publication May 16, 2019;
accepted after revision November 18, 2019.

Published online: November 21, 2019.